Generalization of the phase shift condition in "Intrinsic ICI-free Alamouti Coded FBMC"

Dongjun Na and Kwonhue Choi, *Senior Member, IEEE*

***Abstract*—The condition given in the equation (5) of the paper "Intrinsic ICI-free Alamouti Coded FBMC" accomplishes the desired property, i.e., ICI-free performance of frequency reversal Alamouti coded FBMC. However, this condition is sufficient but not necessary as it corresponds to a subset of the solutions. We show that this condition can be relaxed to cover more general solutions. This generalization allows more beneficial waveform generation such as decoupling peak power minimization at the two TX antennas and no need of null insertion to the center subcarrier.**

***Index Terms*—FBMC (filter bank multicarrier), Alamouti code, Offset QAM (OQAM), PAPR (peak to average power ratio).**

I. Relaxation of the condition given in the equation (5) of [1]

The main goal of this letter is two-folded. First, we aim to provide the generalized version of the equation (5) of [1] which is the phase shift condition for intrinsic ICI-free Alamouti-coded FBMC. Secondly, we show that this generalization brings the substantial benefits to the system if properly exploited.

We inherit the notations and mathematical terms in [1] without introduction for a compact presentation. For the details and the background, refer to the details in [1]. In the equations (2) and (3) in [1], the term $\zeta_{l,m}$ refers to the phase shift term alternating between 1(or -1) and j(or -j) in both of time and frequency axes to form the OQAM signal from the real valued data sequences, $x_{k,n}$ and $y_{k,n}$. It was claimed in [1] that $\zeta_{l,m}$ in the right half subcarriers, i.e., $\zeta_{N_F-l,m}$ for $1 \le l \le N_F/2-1$ should be set to the conjugate of their frequency reversal counter parts in the left half subcarrier, i.e.,

$$\zeta_{N_F-l,m} = \zeta_{l,m}^{*} \text{ for } 1 \le l \le N_F/2-1. \tag{1}$$

This requirement was set up under a constrain that both TX (transmit) antennas use the identical $\zeta_{l,m}$. However, it is found that this constraint is unnecessary and (1) can be relaxed as follows:

$$\zeta_{N_F-l,m}^{(a)} = \chi\zeta_{l,m}^{*(b)} \text{ for } 1 \le l \le N_F/2-1, \tag{2}$$

$$\zeta_{N_F-l,m}^{(b)} = \chi\zeta_{l,m}^{*(a)} \text{ for } 1 \le l \le N_F/2-1. \tag{3}$$

This research was supported in part by Basic Science Research Program through the National Research Foundation (NRF) (2015R1D1A3A01015970) funded by the Ministry of Education, Korea, the ITRC(Information Technology Research Center) support program (IITP-2016-R2718-16-0035) supervised by the IITP(Institute for Information & communications Technology Promotion) funded by the Ministry of Science, ICT and Future Planning, Korea, and the 2017 Yeungnam University Research grant.

The authors are with the Department of Information and Communication Engineering, Yeungnam University, Gyeongsan 38541, South Korea (e-mail: nadj2964@ynu.ac.kr; gonew@yu.ac.k). Corresponding author: Kwonhue Choi.

Moreover, χ is not necessarily 1 but an arbitrary complex number on unit circle, i.e., $|\chi| = 1$. The condition in (2) and (3) implies the case that $\zeta_{l,m}$ are not necessarily the same to both TX antennas and thus, we denote $\zeta_{l,m}^{(a)}$ and $\zeta_{l,m}^{(b)}$ as $\zeta_{l,m}$s for TX antenna A and B, respectively. Explaining (2) and (3), $\zeta_{l,m}^{(a)}$ and $\zeta_{l,m}^{(b)}$ can be independently set for $1 \le l \le N_F/2-1$ and their frequency reversal counter parts are the complex conjugates crossing the antennas with an arbitrary phase rotation. Hence, it is straightforward that (1) is a sufficient condition of (2) and (3), i.e., the solution set for (1) is a subset of the solutions for (2) and (3). This generalization is preferable for more beneficial waveform generation. Two beneficial examples are illustrated in Section III.

II. Proof of ICI free performance with (2) and (3)

Except the modification from (1) into (2) and (3), the transmit signal structure is the same as described in [1]. Hence, we skip this part.

From the change of (1) into (2) and (3), $r_{k,n}$ in the equation (7) in [1] is given as two versions, one compensated by $\zeta_{l,m}^{*(a)}$ and the other one compensated by $\zeta_{l,m}^{*(b)}$ as follows:

$$r_{k,n}^{(a)} = \int_{-\infty}^{\infty} r(t)\zeta_{k,n}^{*(a)} p\left(t-\frac{nT}{2}\right) e^{-j\frac{2\pi kt}{T}} dt, \tag{4}$$

$$r_{k,n}^{(b)} = \int_{-\infty}^{\infty} r(t)\zeta_{k,n}^{*(b)} p\left(t-\frac{nT}{2}\right) e^{-j\frac{2\pi kt}{T}} dt. \tag{5}$$

After the typical combining for Alamouti code, the decision variables for the data symbols $x_{k,n}$ and $y_{k,n}$ are given as follows:

$$d_{k,n}^{(x)} = \Re\left[h_a^{*} r_{k,n}^{(a)} + h_b r_{N_F-k,n}^{*(b)}\right], \tag{6}$$

$$d_{k,n}^{(y)} = \Re\left[h_b^{*} r_{k,n}^{(b)} - h_a r_{N_F-k,n}^{*(a)}\right]. \tag{7}$$

The equations (14) and (15) in [1] are accordingly modified as follows:

$$r_{k,n}^{(a)} = h_a \underbrace{\sum_{l=-L}^{L}\sum_{m=-M}^{M} F_{l,m(a\to a)}^{(k,n)} x_{k+l,n+m}}_{\triangleq U} + h_b \underbrace{\sum_{l=-L}^{L}\sum_{m=-M}^{M} F_{l,m(b\to a)}^{(k,n)} y_{k+l,n+m}}_{\triangleq V} + w_{k,n}, \tag{8}$$

$$r_{N_F-k,n}^{(b)} = h_a \underbrace{\sum_{l=-L}^{L}\sum_{m=-M}^{M} F_{l,m(a\to b)}^{(N_F-k,n)} \times (-y_{k-l,n+m})}_{\triangleq W} + h_b \underbrace{\sum_{l=-L}^{L}\sum_{m=-M}^{M} F_{l,m(b\to b)}^{(N_F-k,n)} x_{k-l,n+m}}_{\triangleq Z} + w_{N_F-k,n} \tag{9}$$

Note that the terms U, V, W and Z in (8) and (9) contain the accordingly modified interference coefficients defined as follows:

$$F^{(k,n)}_{l,m(a\to a)} \triangleq F_{l,m}\zeta^{(a)}_{k+l,n+m}\zeta^{*(a)}_{k,n}(-1)^{nl} \quad (10)$$

$$F^{(k,n)}_{l,m(b\to a)} \triangleq F_{l,m}\zeta^{(b)}_{k+l,n+m}\zeta^{*(a)}_{k,n}(-1)^{nl} \quad (11)$$

$$F^{(k,n)}_{l,m(a\to b)} \triangleq F_{l,m}\zeta^{(a)}_{k+l,n+m}\zeta^{*(b)}_{k,n}(-1)^{nl} \quad (12)$$

$$F^{(k,n)}_{l,m(b\to b)} \triangleq F_{l,m}\zeta^{(b)}_{k+l,n+m}\zeta^{*(b)}_{k,n}(-1)^{nl}. \quad (13)$$

Due to the same reason for the Property I in [1], the following properties hold:

$$\Re\left[F^{(k,n)}_{l,m(a\to a)}\right] = \delta_l\delta_m \quad (14)$$

$$\Re\left[F^{(k,n)}_{l,m(b\to b)}\right] = \delta_l\delta_m. \quad (15)$$

Substituting (8) and (9) into (6), we have

$$\begin{aligned} d^{(x)}_{k,n} &= \Re\left[h^*_a(h_aU + h_bV) + h_b(h_aW + h_bZ)^*\right] + n^{(x)}_{k,n} \\ &= |h_a|^2\Re[U] + |h_b|^2\Re[Z^*] + \Re\left[h^*_a h_b(V + W^*)\right] + n^{(x)}_{k,n} \end{aligned} \quad (16)$$

where $n^{(x)}_{k,n} = \Re[h^*_a w_{k,n} + h_b w^*_{N_F-k,n}]$ and denotes the noise component in the decision variable in $d^{(x)}_{k,n}$. Using the property in (14), the term $\Re[U]$ is derived as:

$$\Re[U] = \sum_{l=-L}^{L}\sum_{m=-M}^{M}\delta_l\delta_m x_{k+l,n+m} = x_{k,n} \quad (17)$$

and similarly,

$$\Re[Z^*] = x_{k,n}. \quad (18)$$

The term W^* in (9) is written as follows:

$$\begin{aligned} W^* &= \left[\sum_{l=-L}^{L}\sum_{m=-M}^{M}F^{(N_F-k,n)}_{l,m(a\to b)}\times(-y_{k-l,n+m})\right]^* \\ &= \left[\sum_{l=-L}^{L}\sum_{m=-M}^{M}F^{(N_F-k,n)}_{-l,m(a\to b)}\times(-y_{k+l,n+m})\right]^*. \end{aligned} \quad (19)$$

Meanwhile, by the relaxed condition in (2) and (3) and the property $F_{-l,m} = F^*_{l,m}$, the term $F^{(N_F-k,n)}_{-l,m(a\to b)}$ in (19) is derived as follows:

$$\begin{aligned} F^{(N_F-k,n)}_{-l,m(a\to b)} &= F_{-l,m}\zeta^{(a)}_{N_F-k-l,n+m}\zeta^{*(b)}_{N_F-k,n}(-1)^{-nl} \\ &= F^*_{l,m}\left(\chi\zeta^{*(b)}_{k+l,n+m}\right)\left(\chi^*\zeta^{(a)}_{k,n}\right)(-1)^{nl} \\ &= F^*_{l,m}|\chi|^2\zeta^{*(b)}_{k+l,n+m}\chi\zeta^{(a)}_{k,n}(-1)^{nl} \end{aligned} \quad (20)$$

and then, by the condition $|\chi| = 1$ and (11), we have

$$\begin{aligned} F^{(N_F-k,n)}_{-l,m(a\to b)} &= F^*_{l,m}\zeta^{*(b)}_{k+l,n+m}\chi\zeta^{(a)}_{k,n}(-1)^{nl} \\ &= F^{*(k,n)}_{l,m(b\to a)}. \end{aligned} \quad (21)$$

Substituting (21) into (19),

$$\begin{aligned} W^* &= \left[\sum_{l=-L}^{L}\sum_{m=-M}^{M}F^{*(k,n)}_{l,m(b\to a)}\times(-y_{k+l,n+m})\right]^* \\ &= -\sum_{l=-L}^{L}\sum_{m=-M}^{M}F^{(k,n)}_{l,m(b\to a)}y_{k+l,n+m} = -V. \end{aligned} \quad (22)$$

Consequently, substituting (17), (18) and (22) into (16), we have

$$d^{(x)}_{k,n} = \left(|h_a|^2 + |h_b|^2\right)x_{k,n} + n^{(x)}_{k,n}. \quad (23)$$

By going through the similar derivations,

$$d^{(y)}_{k,n} = \left(|h_a|^2 + |h_b|^2\right)y_{k,n} + n^{(y)}_{k,n}. \quad (24)$$

Note that the signal terms and the noise terms in the decision variables (23) and (24) have the same distributions as the case with the ideal Alamouti decoding, i.e., the ICI-free case. This concludes the proof.

III. The Benefits of the Generalized Condition

A. Decoupling peak power minimization at the two TX antennas

In order to compare the PAPR (peak to average power ratio) performances between the two systems with the previous and the generalized phase shift conditions, respectively, we consider a typical SLM (selective mapping) algorithm[2, 3]. As there is no constraint on the elements' signs of the left half subcarriers' phase shift pattern $\zeta_{1:(N_F/2-1),m}$ $\left(\zeta^{(a)}_{1:(N_F/2-1),m}\right.$ and $\left.\zeta^{(b)}_{1:(N_F/2-1),m}\right.$ for the generalized condition$\Big)$, we prepare the multiple number of phase shift patterns. They are made by element-wise multiplying the different binary sequences consisting of 1 or -1 to the original phase shift pattern. Then, the same remaining process (such as (1) for the previous condition or (2) and (3) for the generalized condition) is performed for each of different phase shift patterns, respectively to generate the corresponding transmit waveforms. Finally, the waveform with the minimum peak power over the two TX antennas is transmitted.

Meanwhile, recall from (2) and (3) that, with the generalized condition, the left half subcarriers' phase shift patterns for the two TX antennas, i.e., $\zeta^{(a)}_{1:(N_F/2-1),m}$ and $\zeta^{(b)}_{1:(N_F/2-1),m}$ do not need to be the same unlike the previous condition in (1). Therefore, they can be independently chosen so that they minimize the peak powers of TX antenna A and TX antenna B, respectively. In other words, the peak power minimizations of the two TX signals are decoupled and thus, the degree of freedom for the peak minimization is higher compared to the case with the previous condition. This leads us to expect the reduced PAPR by the generalized condition.

Fig. 1 confirms this expectation. It shows the peak power's CCDF (complementary cumulative distribution function) curves when the number of candidates U = 8 and N_F= 16 and 32, respectively. It is shown that the case with the generalized phase shift condition in (2) and (3) achieves the substantially reduced PAPR compared to the case with the previous condition in (1).

B. No need of null insertion

According to the condition in (1), the ζs for each frequency reversal subcarrier pair are complex conjugate each other and thus, they should be one of (1,1), (-1,-1) (j,-j) or (-j, j). Also, this holds for the closest pair (the last subcarrier of the left half band, the first subcarrier of the right half band) that meets at the middle of frequency band. Meanwhile, note that according to the basic requirement for FBMC modulation given in the equation (4) of [1], ζ alternates between 1 (or -1) and j (or -j) in time and frequency axes and thus it is impossible that ζs

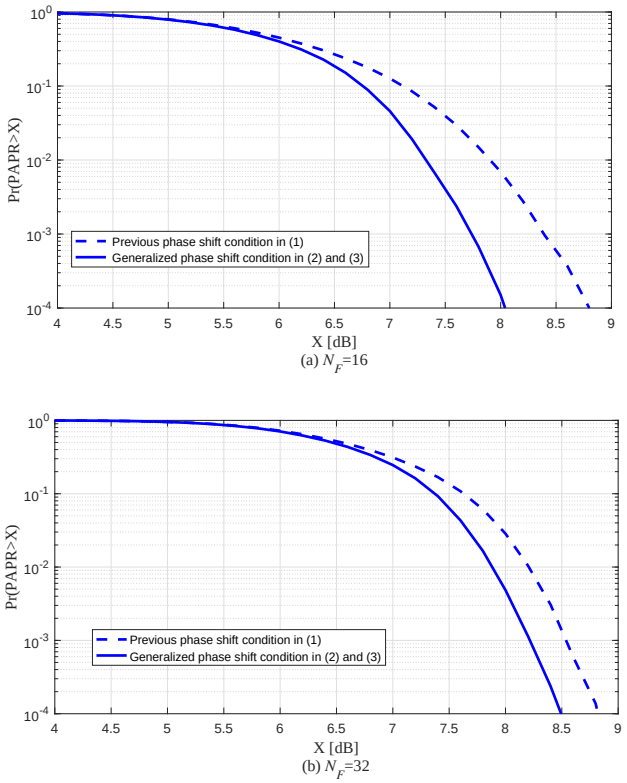

Fig. 1. The CCDF curves of PAPR for U=8, N_F=16 and 32.

for the consecutive subcarriers are both real or both imaginary. In order to avoid the contradiction of the two requirements mentioned above, the closest frequency reversal subcarrier pairs cannot be the consecutive one. This is why the null should be inserted to the center subcarrier, i.e., in the $N_F/2$-th subcarrier and the subcarrier indices for the closest frequency reversal subcarrier pairs are set $N_F/2-1$ and $N_F/2+1$.

On the other hand, in the relaxed condition in (2) and (3), we have an extra variable χ by which we can avoid the contradiction mentioned above. More specifically, if we set χ to j (or -j), it is straightforward that we can make the ζs of the closest frequency reversal subcarrier pair, i.e., ($\zeta^{(a)}_{N_F/2-1}$, $\zeta^{(a)}_{N_F/2+1}$) or ($\zeta^{(b)}_{N_F/2-1}$, $\zeta^{(b)}_{N_F/2+1}$) in (2) and (3) be (real, imaginary) or (imaginary, real). Moreover, then, the closest frequency reversal subcarrier pair can be placed next each other in the subcarrier axis satisfying FBMC signal format. In other words, we do not need to leave the center ($N_F/2$-th) subcarrier as a null. Therefore, if we take χ = j (or -j), the requirement in (2) and (3) can be modified as follows:

$$\zeta^{(a)}_{N_F-l+1,m} = \chi\zeta^{*(b)}_{l,m} \text{ for } 1 \le l \le N_F/2, \quad (25)$$

$$\zeta^{(b)}_{N_F-l+1,m} = \chi\zeta^{*(a)}_{l,m} \text{ for } 1 \le l \le N_F/2. \quad (26)$$

Note that unlike (1), (2) and (3), the range of the half band subcarrier index l in (25) and (26) now includes the center ($N_F/2$-th) subcarrier and its frequency reversal pair is the $N_F/2+1$-st subcarrier which is the very next one in the subcarrier axis. This means no null subcarrier in the center.

Fig. 2 shows the simulated BER (bit error rate) results for the case with the modified condition in (25) and (26) for $N_F = 16$ and $N_F = 32$, respectively. The simulated multipath channel is the ITU-R Pedestrian-A model[4]. The parameters for the system and the channel model are identical to those in [1]. For reference, the case with the previous condition in (1) is included. The two cases achieve the very close BER levels. This is because the modified condition has no intra-antenna ICI even without null subcarrier insertion as proved in Section II. Meanwhile, despite no intra-antenna ICI, there exists a residual inter-antenna ICI only between $N_F/2$th subcarrier of one antenna and $N_F/2+1$-th subcarrier of the other antenna because the received signals from the two TX antennas undergo the independent phase rotations. This explains the slight BER increases in the high SNR region compared to the reference case.

Note that the case with the modified condition achieves full data rate because of no null subcarrier. On the other hand, the reference case has the data rate loss of $1/(N_F-1)$ (= 6.6 % and 3.2 % for $N_F = 16$ and $N_F = 32$, respectively) because of one null subcarrier out of N_F-1 subcarrier positions in total. Hence, for comparison under the same data rate basis in Fig. 2, we also include another case when the previous condition in (1) is employed but the center carrier (=$N_F/2$-th subcarrier) is not a null but forced to carry the data and thus,the condition in (1) is accordingly modified to include $N_F/2$-th subcarrier as follows:

$$\zeta_{N_F-l+1,m} = \zeta^{*}_{l,m} \text{ for } 1 \le l \le N_F/2. \quad (27)$$

Compared to the case with the modified condition, the case with the condition in (27) has the severely increased BER in the high SNR region. This is due to the fact that ζ for the consecutive subcarriers in the center, i.e., ($\zeta_{N_F/2}, \zeta_{N_F/2+1}$) are both real or both imaginary and this breaks the FBMC signal format as we mentioned above.

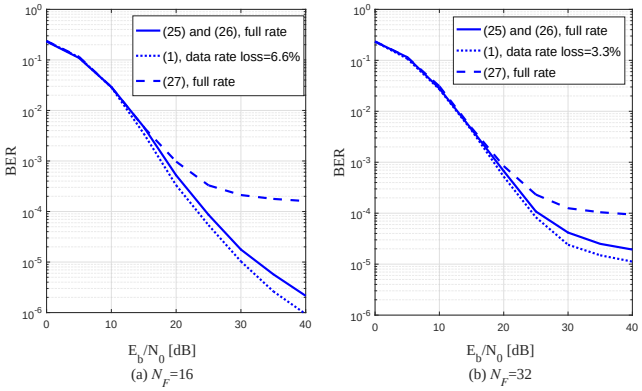

Fig. 2. The BER curves for the three different phase shift conditions.

In short, we have confirmed another benefit by the relaxed condition in (2) and (3). Basically, it enables a further modification into (25) and (26) and then, the modified condition allows the removal of the null data in the center subcarrier while maintaining the BER performance close to the ICI-free case. On the other hand, in the previous condition in (1),

if the null subcarrier is removed as given in (27), the BER performance severely deteriorates. Consequently, the modified condition is a reasonable solution in terms of both BER performance and bandwidth efficiency.

REFERENCES

[1] D. Na and K. Choi, "Intrinsic ICI-Free Alamouti Coded FBMC," *IEEE Communications Letters*, vol. 20, no. 10, pp. 1971-1974, Oct. 2016.

[2] Mounira Laabidi, Rafik Zayani and Ridha Bouallegue, "A novel multi-block selective mapping scheme for PAPR reduction in FBMC/OQAM systems," *IEEE World Congress on Information Technology and Computer Applications Congress (WCITCA)* 2015.

[3] S. S. Krishna Chaitanya Bulusu, et al., "Reduction of PAPR for FBMC-OQAM systems using dispersive SLM technique," *IEEE International Symposium on Wireless Communications Systems (ISWCS)*, 2014.

[4] *Guidelines for Evaluation of Radio Transmission Technologies for IMT-2000*, document ITU-R M.1225, 1997.